Aquaculture and Coastal Habitats Report No. 2

Mapping Vulnerability and Risk of Land Conversion for Pond Aquaculture in Thailand, Cambodia and Vietnam

Sean Cunningham, J. Ronald Eastman and Stefano C. Crema

Clark Labs, Clark University

Abstract
Aquaculture is the fastest growing agriculture sector and now produces more seafood than wild-caught fisheries. Growth has been especially strong in Southeast Asia with shrimp production in Thailand, Cambodia and Vietnam accounted for 20% of global supply in 2012. Conversion of lands for brackish water pond aquaculture for the shrimp industry has had a significant impact on coastal and near-shore environments, particularly mangrove forests. The goal of this study was to assess current vulnerability to conversion to pond aquaculture in the coastal zones of Thailand, Cambodia and Vietnam, and subsequently to map the probability of conversion by 2050. Landsat TM data from 1988-1990 were used to map areas of pond aquaculture, mangroves, cropland, stabilized sand and sea salt production. These were compared to a map of the same categories for 2013-2015 using Landsat 8 data and the same methodologies (Eastman et al., forthcoming). Historical transitions between pond aquaculture and the other categories were then used along with a set of explanatory variables (elevation, proximity to the coast, proximity to pond aquaculture in 1988-1990, and Landsat TM bands 1-5 and 7 from 1988-1990) to empirically model vulnerability. The measure of vulnerability used was a Multi-Layer Perceptron output activation level. These vulnerability maps were then transformed into risk maps expressing the probability of conversion of lands in 2013-2015 by 2050. These maps are provided at a 15 m resolution and intended for province and district level planning. Validation data indicated that the models had a mean skill of 0.61 translating to an accuracy of 81%. Based on the risk mapping, estimates can be made of further conversions to 2050. These estimates assume that the rates of transition experienced at the provincial level over the past 25 years will continue until 2050. Cambodia has very little pond aquaculture and thus no significant conversions of mangroves or cropland are projected (less than 1 km^2 each). Thailand is expected to see a further loss of 142.80 km^2 of mangroves, 963.72 km^2 of cropland and 13.66 km^2 of salt production to pond aquaculture area if past trends of pond development continue. For Vietnam, the projection of past trends indicates a further loss to pond aquaculture of 299.99 km^2 of mangrove, 2727.52 km^2 of cropland, 7.58 km^2 of stabilized sand and 14.35 km^2 of sea salt production areas by 2050. Note, however, that these figures represent land cover conversions and not changes in net area.

Introduction
Aquaculture is the fastest growing agricultural sector, globally, and shrimp aquaculture is favored as a means to alleviate poverty and shrinking wild-caught fisheries (Béland et al., 2006; Brakel and Ross, 2010). Since the mid-1970s global mangrove deforestation attributed to shrimp aquaculture has destroyed an estimated 5,440 km^2 of marine and terrestrial

habitat while contributing to atmospheric carbon dioxide, and increasing coastal erosion and soil salinization (Barbier and Cox, 2004; Siikamäki et al., 2012; Hamilton, 2013; Jones et al., 2014). Shrimp aquaculture in the coastal area of Southeast Asia (Cambodia, Thailand, and Vietnam) accounted for 20% of the 4.5 million tonnes produced globally in 2013 (FISHSTAT 2015).

Unplanned and poorly managed shrimp aquaculture has negative impacts on terrestrial and marine environments including eutrophication, land degradation, and land-use conflicts (Lebel et al., 2002; Barbier and Cox, 2004). While shrimp farming can be more profitable than traditional forms of agriculture, brackish water pond aquaculture constructed on agricultural land is often practiced unsustainably resulting in water pollution and land degradation through organic and chemical effluents and soil salinization (Barbier and Cox, 2004; Szuster, 2006). Shrimp farming can be practiced sustainably while simultaneously increasing productivity by regulating ponds to locations with previously degraded land, appropriate soil salinity and drainage infrastructure. However, this is rarely practiced (IUCN, 2003; Szuster, 2006).

As land is converted to pond aquaculture it is important to regionally plan conversion in order to protect coastal ecosystems and the livelihoods of residents, as well as reduce land-use conflicts (Lebel, et al., 2002; McLeod et al., 2002; Giap et al., 2005; Szuster, 2006; Hossain and Das, 2010). In order to assess its impact, measurements of the proportion of land converted to pond aquaculture are needed, particularly mangrove and cropland (Dahdouh-Guebas et al., 2002; Dung et al., 2009; Hamilton, 2015). Regional-scale information on land-cover change and transition potential to pond aquaculture would improve government planning of future land conversion and habitat conservation (Lebel et al., 2002; Vo et al., 2013).

This study models, maps and evaluates the vulnerability of coastal land-cover for conversion to pond aquaculture in Thailand, Cambodia and Vietnam and the risk of conversion by 2050. Vulnerability expresses the readiness of land to transition for reasons related to the suitability of the land and its context. Risk, on the other hand, is a function of both vulnerability and exposure (Cardona, 2003), which in this case relates to the expected rate of change. Using Landsat Thematic Mapper (TM) data from 1988-1990 areas of pond aquaculture, mangrove, cropland, stabilized sand, and salt production were mapped. This along with a recent mapping of land cover based on Landsat 8 Operational Land Imager (OLI) data from 2013-2015 (Eastman et al., forthcoming) allowed the determination of the locations and rates of change. Using a set of explanatory variables, a Multi-Layer Perceptron (MLP) neural network was used to model the vulnerability of transition from each of mangrove, cropland, stabilized sand and salt production to pond aquaculture. These in turn were used with calculated rates of change to estimate the risk of transition up to the year 2050.

Study Area

The study described here was a planned follow-on to the baseline mapping of aquaculture and coastal habitats for the coastal zone of Thailand, Cambodia and Vietnam described in Eastman et al., (forthcoming). The project was conducted on behalf of the Gordon and Betty Moore Foundation in support of its Marine Conservation Initiative. Thailand and Vietnam are among the five largest producers of shrimp worldwide (FAO, 2014) and have experienced significant loss of mangrove forests for the construction of shrimp ponds. In comparison, Cambodia has relatively little brackish water pond aquaculture. However, it has important mangrove resources that face many threats, including destruction for the purpose of farming shrimp (Song, 2004).

As defined by Eastman et al. (forthcoming), the coastal zone was established as

> a zone 10 km on either side of the coastline. Where necessary, the zone was extended to include marine areas <= 30 m based on the GEBCO (2010) bathymetry and land areas <= 5 m as defined by the SRTM (2009) elevation data. The main areas affected by these extensions were the Red and Mekong river deltas in Vietnam and the Chao Phraya river basin in Thailand. Based on information related to salt intrusion in these regions (Anh Duc, 2008; Arli, 2007; Vu and Bui, 2006), a maximum extension of 60 km inland from the coast was allowed. The primary concern was to limit the inland extent to areas where it was likely that pond aquaculture would be dominated by brackish water and thereby have a stronger likelihood of being used for shrimp.

In total, the coastal zone overlapped 42 Landsat scenes.

Data

For the 1988-1990 mapping, a total of 30 geometrically corrected Landsat-TM scenes were used, chosen for minimal cloud-cover and overlap with the defined coastal zone (Table S1 in the supporting materials, at www.clarklabs.org/downloads/TCV_vulnerability). The number is smaller than the 42 mentioned above because some images have so little overlap with the coastal zone that an inadequate sample would be available for modeling. Following cloud and shadow removal with the *Fmask* automated cloud masking software (Zhu et al., 2015), all images were corrected for solar elevation angle, haze (using Dark Object Subtraction), converted to ground reflectance and masked to the study area (Chavez, 1996).

For explanatory variables the following layers were acquired or developed:

1. 30 m spatial resolution elevation data from the Shuttle Radar Topography Mission (SRTM) (Farr et al., 2007).
2. Proximity to the coast in 1988-1990.
3. Proximity to pond aquaculture in 1988-1990.
4. 1988-1990 Landsat TM Bands 1-5 and 7.

The elevation and proximity to coast variables represent accessibility to brackish water (Giap et al., 2005). The proximity to existing pond aquaculture variable is included because a previous study found existing shrimp farms to be a positive influence on conversion area (Abdus Salam et al., 2003). The TM reflectance bands were included as a proxy for biophysical variables such as soil moisture, soil composition and land cover (Rogan and Yool, 2001). Biophysical indicators directly influence site selection and productivity of pond aquaculture (McLeod et al., 2002).

Methods

Classification of the historical (1988-1990) imagery for mangroves, cropland, stabilized sand, and salt production was achieved with a Mahalanobis Typicality classifier (Foody, et al., 1992) in the *TerrSet* software system (Eastman, 2015). Mahalanobis Distance measures class membership based on multivariate distance from the class mean (Li and Fox, 2010). Mahalanobis typicality is the probability of a given value having a Mahalanobis Distance less than all other possible values (Foody et al., 1992). Mahalanobis typicality outputs a soft classification ranging from 0-1; a value of 1 indicates perfect membership to the class mean from which it was trained. Mahalanobis typicality was used for this study because of its capability to classify one class at a time; no *a priori* knowledge of all land-cover classes is required (Li and Fox, 2010). This permitted classification of only at-risk land-cover classes with a Mahalanobis typicality ≥ 0.05 and further reduced the spatial extent of the Landsat data.

All aquaculture ponds were manually delineated from the historical Landsat TM data using visual comparison of natural and false-color composites with high spatial resolution imagery in *Google Earth*. False color composites of Landsat TM bands 4 as red, 7 as green, and 3 as blue work well for displaying pond aquaculture, cropland and mangrove.

The procedure used to do the vulnerability analysis was the Multi-Layer Perceptron (MLP) in the *Land Change Modeler* (LCM) component of the *TerrSet* system (Eastman, 2015). LCM takes a pair of land cover layers from different dates as inputs and offers the ability to model user-specified transitions using a set of explanatory variables. The output of MLP is a transition potential map with pixel values than range from 0-1. In normal use, these transition potentials serve as inputs to a spatial allocation process that produces a land cover prediction for a specified future date. However, in this context, the transition potential is an expression of vulnerability.

The implementation of MLP in LCM takes all (or a sample of) pixels that experienced the transition being modeled (*change*) and an equal size sample of those that were eligible to transition, but which did not (*persistence*). By default, it sets the maximum sample size to 10,000 pixels of each. It then randomly assigns half of each sample to be used for training and half for validation. From this it can compute the skill of the model.

The use of equal size samples is known as *case-control* sampling and is important in Logistic Regression with rare event data (King and Zeng, 2001a; 2001b). Weiss (2004) has shown that it is also important for data mining applications. In the case of MLP, it is essential to developing a balanced network. In land change modeling, the quantity of land that changes between two dates is typically very small compared to the quantity that persists. If case-control sampling weren't done, the network would focus primarily on modeling persistence.

Because of the use of case-control sampling, the transition potentials have a special character. Technically, they are the activation levels of the output neurons, one neuron per class. As indicated by Hsieh (2009), the output activation levels are in fact posterior probabilities. However, since case-control sampling was used, they are effectively the posterior probabilities assuming equal prior probabilities for change and persistence. Effectively, then, it's a statement of potential without consideration of the relative probabilities of change or persistence. This is very much the character of an expression of vulnerability.

To convert this statement of vulnerability into a statement of risk requires what is known as prior-correction. King and Zeng (2001a) discuss the procedure for prior-correction with logistic regression but note that it is appropriate for any model with a logit output such as

MLP. In the context of logistic regression, the procedure involves correction of the intercept. However, it can be shown that when the original model is based on equal prior probabilities, the formula simplifies to:

$$\mathrm{p}=\frac{\mathrm{k}}{1+\mathrm{k}} \text{ where } k = \left(\frac{v}{1-v}\right)\left(\frac{c}{1-c}\right) \qquad (1)$$

Where *p* is the prior-corrected posterior probability of change, *v* is the vulnerability (transition potential) determined with case-control sampling and *c* is the correct prior probability of change.

In the case of an estimation of future risk, the correct "prior" probability is actually the rate of change expected between the second land cover image and the future date. In this study, the later land cover map was from 2013-2015 and is thus considered to centrally represent 2014. The earlier land cover is from 1988-1990 and is considered to represent 1989. Thus it is considered that there are 25 years between the two land cover images and 36 years between the later one and a future prediction date of 2050.

In this study, it is assumed that the rate of change remains constant from one time interval to the next. Such a basis is Markovian (Grimstead and Snell, 1997) where the change from one moment to the next is only dependent on the previous state and a fixed transition probability from step to step. The procedure here is to use the 25 year historical rate of change to estimate the annual rate of change and then use that rate to project the ensuing 36 years of change.

To calculate the 25-year historical rate the two land cover maps were masked to remove areas that were covered by clouds in either image. The areas of mangrove, cropland, stabilized sand and salt production that changed to pond aquaculture in 2013-2015 were then divided by the areas of those classes in 1988-1990 to derive the historical rates of change.

The procedure for determining the annual rate of change from the 25-year historical rate was as follows:

$$a = 1 - (1 - h)^{1/n} \qquad (2)$$

where *h* is the historical rate of change and *n* is the number of intervening years. The future rate of change is determined as:

$$f = 1 - (1 - a)^{n} \qquad (3)$$

where *n* in this case is the number of years being projected into the future.

Because of the double masking for clouds across the two dates, the areas of categories used to calculate rates is smaller than the 2013-2015 values. As a result, any figures that relate to change are expressed as rates. Any figures that express areas come from the 2013-2015 data without masking.

Results

Table 1 shows the areas of pond aquaculture by country in 2013-2015 as well as the percentage change from 1988-1990 broken down by country. It also indicates the relative contribution of each of the four cover types of focus, expressed as a percent. Finally, Table 1 shows the percent loss of land for each of the four focus covers as a result of conversion to pond aquaculture. Note that these figures do not account for conversions from pond back to one these four covers. Thus the loss percentage expresses the degree of disturbance over the 25 year period.

Thailand experienced an increase of 123.04% from 1988-1990 to 2013-2015, with most of it (90.49%) coming from cropland. The contribution of mangrove was much smaller (7.70%). Salt production contributed less than 2%, but its level of disturbance was highest with over 21% loss.

Cambodia has a very small amount of pond aquaculture so the percentage change and contribution/loss figures are not particularly meaningful.

Vietnam experienced an enormous change with 700.47% growth in area over the 25 year period. The main contributor was cropland (87.60%). However, the percent loss of cropland was only 14.54% compared to 45.95% for mangrove. Thus the impact on mangroves was proportionally far greater than cropland.

Over the region as a whole, there are 10484.27km^2 of pond aquaculture in 2013-2015 (including integrated mangrove-shrimp) which represents a 414.69% increase since 1988-1990.

Table 1

	Area of Pond Aquaculture* 2013-2015 (km^2)	% Change from 1988-1990	% Contribution to Pond Aquaculture (% Loss of Land)			
			Mangrove	Cropland	Stabilized Sand	Salt Production
Thailand	2080.71	123.04%	7.70% (4.92%)	90.49% (5.40%)	0% (0%)	1.82% (21.37%)
Cambodia	9.16	2529.13%	26.04% (0.72%)	73.96% (0.19%)	0% (0%)	0% (0%)
Vietnam	8395.03	700.47%	9.79% (45.95%)	87.60% (14.54%)	0.23% (3.90%)	2.38% (66.91%)
Region	10484.27	414.69%	9.45% (20.72%)	88.07% (11.00%)	0.19% (3.90%)	2.28% (52.25%)

* Includes ponds associated with integrated mangrove shrimp

Based on the rates of change over 25 years, annual rates of change were calculated using equation 2 above. The results are indicated in Table 2.

Table 2: Annual rates of transition to Pond Aquaculture

	Cropland	Mangrove	Stabilized Sand	Salt Production
Thailand	0.002218	0.002014	0	0.009569
Cambodia	0.000075	0.000287	0	0
Vietnam	0.006266	0.024313	0.001591	0.043269
Region	0.004649	0.009246	0.001591	0.029135

Using the two land cover maps for 1989-1990 and 2013-2015, the Land Change Modeler system in TerrSet (Eastman, 2015) was used to model vulnerability to pond conversion for each of the four land covers of focus. Modeling was done on a scene by scene basis since the rationale for change likely varies for different locations. A total of 57 Multi-Layer Perceptron models were run with the number per scene varying from 1 to 4 depending upon which transitions were present. Table 3 summarizes the mean skill of the models for each of the four transitions as well as overall. The skill measure is a Peirce Skill Score which ranges from -1 to +1 with 0 indicating skill no better than random. The skill levels were generally similar with an overall value of 0.62. Expressed as an accuracy, this is equivalent to an accuracy rate of 81% in predicting whether a pixel will transition or not.

Table 3: Mean model skill by the type of transition.

Transition	Mean Skill Change	Mean Skill Persistence	Mean Skill Overall	Equivalent Accuracy
Pond to Mangrove	0.58	0.53	0.56	78%
Pond to Cropland	0.73	0.64	0.68	84%
Pond to Stabilized Sand	0.63	0.61	0.62	81%
Pond to Salt Production	0.54	0.56	0.55	78%
Overall	0.66	0.59	0.62	81%

Figure 1 shows an illustration of the modeled vulnerability of mangroves to pond conversion in the vicinity of the Pak Phanang district of Nakhon Si Thammarat Province in Thailand as well as areas of existing pond aquaculture in 2013-2015. Figure 2 shows a risk map for the year 2050 using the provincial-level annual rate of conversion of mangrove to pond aquaculture of 0.56% per annum. Vulnerability and risk maps for each country can be found in the supporting materials.

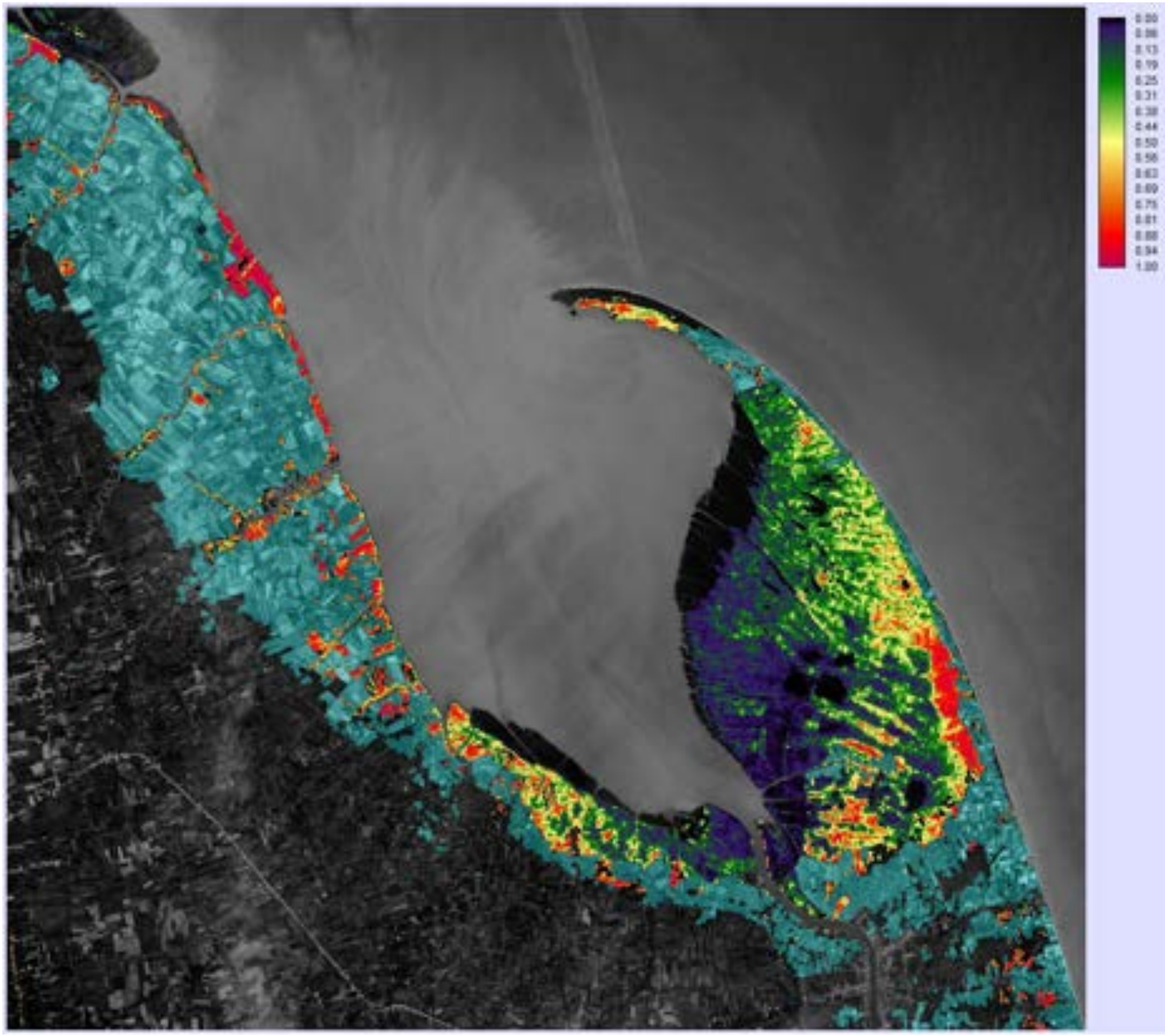

Figure 1: Modeled vulnerability of conversion from mangrove to pond aquaculture in the vicinity of the Pak Phanang district of Nakhon Si Thammarat Province in Thailand. Light blue (cyan) areas are existing pond aquaculture in 2013-2015.

One of the interesting features of the risk map is that the sum of the probabilities in any region will indicate the expected quantity of change. Tables 4, 5 and 6 indicate the mean vulnerability, mean risk and expected area of change by 2050 for each province of Thailand, Cambodia and Vietnam respectively. Note that the risk maps were created using rates of change calculated at the provincial level. Also note that the expected areas of change are likely to be underestimates since areas covered by clouds in either 1988-1990 or 2013-2015 (where the land cover is unknown) are not accounted for. However, the areas tabulated provide a sense of the magnitude of expected change.

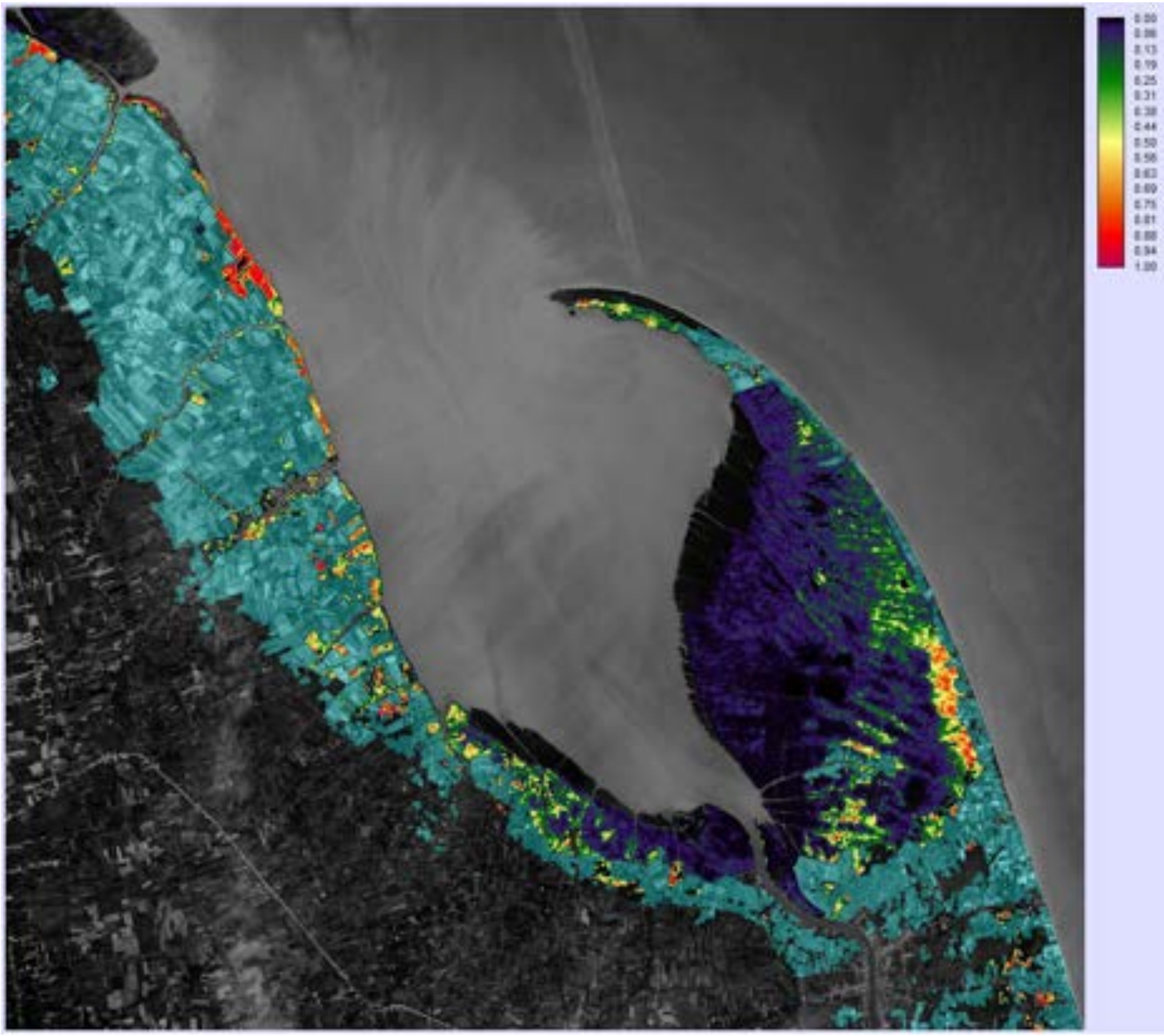

Figure 2: Estimated risk of conversion from mangrove to pond aquaculture in 2050 using the annual provincial-level arte of 0.56% per annum in the vicinity of the Pak Phanang district of Nakhon Si Thammarat Province in Thailand. Light blue (cyan) areas are existing pond aquaculture in 2013-2015.

Table 4: Vulnerability, Risk and Expected Change for Conversion to Pond Aquaculture in Thailand.

Mangrove	Province Name	Mean Vulnerability	Mean Risk	Expected Change by 2050 (km2)
	Bangkok	0.5378	0.0927	0.07
	Chachoengsao	0.4042	0.0188	0.20
	Chanthaburi	0.4412	0.1973	14.43
	Chonburi	0.4225	0.0136	0.09

	Chumphon	0.3166	0.1484	6.15
	Krabi	0.2785	0.0364	13.15
	Nakhon Nayok	0.0000	0.0000	0.00
	Nakhon Pathom	0.0000	0.0000	0.00
	Nakhon Si Thammarat	0.3462	0.1699	17.80
	Narathiwat	0.0000	0.0000	0.00
	Nonthaburi	0.0000	0.0000	0.00
	Pathum Thani	0.0000	0.0000	0.00
	Pattani	0.1299	0.0155	0.19
	Phang Nga	0.2359	0.0104	3.97
	Phatthalung	0.4515	0.0935	0.01
	Phatthalung (Songkhla Lake)	0.3758	0.0113	0.00
	Phetchaburi	0.3490	0.0412	0.69
	Phra Nakhon Si Ayutthaya	0.0000	0.0000	0.00
	Phuket	0.2807	0.0713	0.89
	Prachinburi	0.0000	0.0000	0.00
	Prachuap Khiri Khan	0.3977	0.4174	0.36
	Ranong	0.2147	0.0020	0.01
	Ratchaburi	0.0000	0.0000	0.00
	Rayong	0.4759	0.2920	1.79
	Samut Prakan	0.4591	0.0281	0.37
	Samut Sakhon	0.5360	0.0332	0.40
	Samut Songkhram	0.4198	0.0347	0.71
	Satun	0.2429	0.0293	5.16
	Songkhla	0.4562	0.2254	0.19
	Songkhla (Songkhla Lake)	0.4841	0.0000	0.00
	Surat Thani	0.5961	0.5197	49.97
	Trang	0.2994	0.0540	18.14
	Trat	0.3103	0.0876	8.06
	All Thailand	0.3042	0.0765	142.80

Cropland	Province Name	Mean Vulnerability	Mean Risk	Expected Change by 2050 (km2)
	Bangkok	0.3503	0.0290	17.54
	Chachoengsao	0.4535	0.1494	221.18
	Chanthaburi	0.1522	0.0174	8.06
	Chonburi	0.3711	0.1738	48.37
	Chumphon	0.1567	0.0125	12.77
	Krabi	0.2123	0.0249	17.38
	Nakhon Nayok	0.5646	0.0909	13.48
	Nakhon Pathom	0.2442	0.0306	29.23
	Nakhon Si Thammarat	0.1458	0.0192	36.05

	Narathiwat	0.0002	0.0000	0.00
	Nonthaburi	0.2721	0.0015	0.52
	Pathum Thani	0.3755	0.0097	9.09
	Pattani	0.2330	0.0272	15.85
	Phang Nga	0.2885	0.0330	9.72
	Phatthalung	0.0558	0.0005	0.30
	Phatthalung (Songkhla Lake)	0.1340	0.0061	0.01
	Phetchaburi	0.2431	0.0437	31.52
	Phra Nakhon Si Ayutthaya	0.4701	0.0095	0.50
	Phuket	0.3926	0.0674	2.46
	Prachinburi	0.6274	0.3984	77.27
	Prachuap Khiri Khan	0.1868	0.0405	39.06
	Ranong	0.1624	0.0207	9.56
	Ratchaburi	0.2834	0.0403	28.40
	Rayong	0.1312	0.0087	2.85
	Samut Prakan	0.4584	0.3528	87.02
	Samut Sakhon	0.4658	0.1972	61.94
	Samut Songkhram	0.4485	0.1792	33.29
	Satun	0.3595	0.1348	25.56
	Songkhla	0.3200	0.0599	57.40
	Songkhla (Songkhla Lake)	0.2981	0.0484	0.05
	Surat Thani	0.1554	0.0385	32.78
	Trang	0.2198	0.0401	30.03
	Trat	0.1031	0.0084	4.47
	All Thailand	0.2572	0.0544	963.72

Salt	Province Name	Mean Vulnerability	Mean Risk	Expected Change by 2050 (km2)
	Bangkok	0.0000	0.0000	0.00
	Chachoengsao	0.5920	0.7564	0.66
	Chanthaburi	0.0000	0.0000	0.00
	Chonburi	0.0000	0.0000	0.00
	Chumphon	0.0000	0.0000	0.00
	Krabi	0.0000	0.0000	0.00
	Nakhon Nayok	0.0000	0.0000	0.00
	Nakhon Pathom	0.0000	0.0000	0.00
	Nakhon Si Thammarat	0.0000	0.0000	0.00
	Narathiwat	0.0000	0.0000	0.00
	Nonthaburi	0.0000	0.0000	0.00
	Pathum Thani	0.0000	0.0000	0.00
	Pattani	0.0000	0.0000	0.00
	Phang Nga	0.0000	0.0000	0.00

	Phatthalung	0.0000	0.0000	0.00
	Phatthalung (Songkhla Lake)	0.0000	0.0000	0.00
	Phetchaburi	0.1737	0.0172	0.44
	Phra Nakhon Si Ayutthaya	0.0000	0.0000	0.00
	Phuket	0.0000	0.0000	0.00
	Prachinburi	0.0000	0.0000	0.00
	Prachuap Khiri Khan	0.0000	0.0000	0.00
	Ranong	0.0000	0.0000	0.00
	Ratchaburi	0.0000	0.0000	0.00
	Rayong	0.0000	0.0000	0.00
	Samut Prakan	0.3927	0.9996	0.02
	Samut Sakhon	0.4093	0.2933	10.96
	Samut Songkhram	0.4119	0.1410	1.58
	Satun	0.0000	0.0000	0.00
	Songkhla	0.0000	0.0000	0.00
	Songkhla (Songkhla Lake)	0.0000	0.0000	0.00
	Surat Thani	0.0000	0.0000	0.00
	Trang	0.0000	0.0000	0.00
	Trat	0.0000	0.0000	0.00
	All Thailand	0.3314	0.1818	13.66

Table 5: Vulnerability, Risk and Expected Change for Conversion to Pond Aquaculture in Cambodia.

Mangrove	Province Name	Mean Vulnerability	Mean Risk	Expected Change by 2050 (km2)
	Kampot	0.0178	0.0011	0.01
	Kep	0.0188	0.0000	0.00
	Koh Kong	0.2693	0.0060	0.63
	Preah Sihanouk	0.0014	0.0000	0.00
	Pursat	0.0000	0.0000	0.00
	Svay Rieng	0.0000	0.0000	0.00
	Takéo	0.1460	0.0000	0.00
	All Cambodia	0.2074	0.0046	0.63

Cropland	Province Name	Mean Vulnerability	Mean Risk	Expected Change by 2050 (km2)
	Kampot	0.0337	0.0005	0.40
	Kep	0.1050	0.0000	0.00
	Koh Kong	0.0077	0.0003	0.00
	Preah Sihanouk	0.1649	0.0000	0.00

	Pursat	0.0000	0.0000	0.00
	Svay Rieng	0.0000	0.0000	0.00
	Takéo	0.0027	0.0000	0.00
	All Cambodia	0.0297	0.0003	0.40

Table 6: Vulnerability, Risk and Expected Change for Conversion to Pond Aquaculture in Vietnam.

Mangrove	Province Name	Mean Vulnerability	Mean Risk	Expected Change by 2050 (km2)
	An Giang	0.1848	0.0000	0.00
	Bà Rịa–Vũng Tàu	0.4485	0.6247	3.69
	Bắc Giang	0.0000	0.0000	0.00
	Bạc Liêu	0.4132	0.5689	4.03
	Bắc Ninh	0.0000	0.0000	0.00
	Bến Tre	0.4793	0.6734	51.30
	Bình Định	0.0000	0.0000	0.00
	Bình Dương	0.0000	0.0000	0.00
	Bình Thuận	0.0000	0.0000	0.00
	Cà Mau	0.3124	0.6718	77.73
	Cần Thơ City	0.2307	0.0000	0.00
	Đà Nẵng City	0.0000	0.0000	0.00
	Đồng Nai	0.3491	0.0943	4.79
	Đồng Tháp	0.0042	0.0000	0.00
	Hà Nam	0.9182	0.0000	0.00
	Hà Tây	0.0000	0.0000	0.00
	Hà Tĩnh	0.0000	0.0000	0.00
	Hải Dương	0.0000	0.0000	0.00
	Hải Phòng City	0.3170	0.8038	6.74
	Hậu Giang	0.1152	0.0000	0.00
	Hồ Chí Minh City	0.3353	0.0503	15.96
	Hòa Bình	0.0000	0.0000	0.00
	Hưng Yên	0.0000	0.0000	0.00
	Khánh Hòa	0.2538	0.9821	0.06
	Kiên Giang	0.3404	0.3908	7.95
	Long An	0.2957	0.0000	0.00
	Nam Định	0.4694	0.9646	0.57
	Nghệ An	0.0000	0.0000	0.00
	Ninh Bình	0.0000	0.0000	0.00
	Ninh Thuận	0.5256	0.0000	0.00
	Phú Yên	0.0000	0.0000	0.00
	Quảng Bình	0.0000	0.0000	0.00
	Quảng Nam	0.0000	0.0000	0.00

	Quảng Ngãi	0.0000	0.0000	0.00
	Quảng Ninh	0.3259	0.2596	18.44
	Quảng Trị	0.0000	0.0000	0.00
	Sóc Trăng	0.5381	0.4542	9.52
	Tây Ninh	0.0000	0.0000	0.00
	Thái Bình	0.4861	0.9479	1.69
	Thanh Hóa	0.0000	0.0000	0.00
	Thừa Thiên–Huế	0.0000	0.0000	0.00
	Tiền Giang	0.3471	0.6527	26.96
	Trà Vinh	0.4799	0.6907	70.54
	Vĩnh Long	0.0380	0.0000	0.00
	All Vietnam	0.3664	0.3347	299.99

Cropland	Province Name	Mean Vulnerability	Mean Risk	Expected Change by 2050 (km2)
	An Giang	0.0336	0.0000	0.00
	Bà Rịa–Vũng Tàu	0.1998	0.0775	17.75
	Bắc Giang	0.0120	0.0000	0.00
	Bạc Liêu	0.2699	0.4252	349.16
	Bắc Ninh	0.0029	0.0000	0.00
	Bến Tre	0.4899	0.1797	229.50
	Bình Định	0.1104	0.0200	5.12
	Bình Dương	0.3252	0.0000	0.00
	Bình Thuận	0.1463	0.0171	5.78
	Cà Mau	0.6111	0.8963	346.05
	Cần Thơ City	0.1227	0.0000	0.00
	Đà Nẵng City	0.0882	0.0104	0.63
	Đồng Nai	0.3550	0.0646	18.27
	Đồng Tháp	0.0511	0.0001	0.08
	Hà Nam	0.0152	0.0000	0.00
	Hà Tây	0.0037	0.0000	0.00
	Hà Tĩnh	0.2371	0.0661	25.14
	Hải Dương	0.0316	0.0001	0.06
	Hải Phòng City	0.4309	0.1431	83.65
	Hậu Giang	0.3312	0.0000	0.01
	Hồ Chí Minh City	0.4887	0.2330	62.15
	Hòa Bình	0.0000		0.00
	Hưng Yên	0.0072	0.0000	0.00
	Khánh Hòa	0.1855	0.0602	20.63
	Kiên Giang	0.2671	0.1739	540.41
	Long An	0.3000	0.0467	63.71
	Nam Định	0.2646	0.0095	7.87

	Nghệ An	0.1895	0.0416	9.82
	Ninh Bình	0.1551	0.0000	0.00
	Ninh Thuận	0.0877	0.0156	1.69
	Phú Yên	0.1195	0.0233	7.54
	Quảng Bình	0.2112	0.0282	14.32
	Quảng Nam	0.0870	0.0052	1.34
	Quảng Ngãi	0.1417	0.0126	4.12
	Quảng Ninh	0.3378	0.0677	26.99
	Quảng Trị	0.2325	0.0267	7.60
	Sóc Trăng	0.5759	0.2780	590.25
	Tây Ninh	0.0000	0.0000	0.00
	Thái Bình	0.2534	0.0170	18.09
	Thanh Hóa	0.1422	0.0362	3.24
	Thừa Thiên–Huế	0.2508	0.0593	22.13
	Tiền Giang	0.3130	0.0146	25.76
	Trà Vinh	0.5663	0.1647	218.64
	Vĩnh Long	0.2027	0.0000	0.01
	All Vietnam	0.2690	0.0943	2727.52

Stabilized Sand	Province Name	Mean Vulnerability	Mean Risk	Expected Change by 2050 (km2)
	An Giang	0.0000	0.0000	0.00
	Bà Rịa–Vũng Tàu	0.0000	0.0000	0.00
	Bắc Giang	0.0000	0.0000	0.00
	Bạc Liêu	0.0000	0.0000	0.00
	Bắc Ninh	0.0000	0.0000	0.00
	Bến Tre	0.0000	0.0000	0.00
	Bình Định	0.2986	0.0139	0.14
	Bình Dương	0.0000	0.0000	0.00
	Bình Thuận	0.0000	0.0000	0.00
	Cà Mau	0.0000	0.0000	0.00
	Cần Thơ City	0.0000	0.0000	0.00
	Đà Nẵng City	0.0000	0.0000	0.00
	Đồng Nai	0.0000	0.0000	0.00
	Đồng Tháp	0.0000	0.0000	0.00
	Hà Nam	0.0000	0.0000	0.00
	Hà Tây	0.0000	0.0000	0.00
	Hà Tĩnh	0.0000	0.0000	0.00
	Hải Dương	0.0000	0.0000	0.00
	Hải Phòng City	0.0000	0.0000	0.00
	Hậu Giang	0.0000	0.0000	0.00
	Hồ Chí Minh City	0.0000	0.0000	0.00

	Hòa Bình	0.0000	0.0000	0.00
	Hưng Yên	0.0000	0.0000	0.00
	Khánh Hòa	0.3629	0.0760	0.80
	Kiên Giang	0.0000	0.0000	0.00
	Long An	0.0000	0.0000	0.00
	Nam Định	0.0000	0.0000	0.00
	Nghệ An	0.0000	0.0000	0.00
	Ninh Bình	0.0000	0.0000	0.00
	Ninh Thuận	0.0000	0.0000	0.00
	Phú Yên	0.2497	0.0341	0.80
	Quảng Bình	0.2929	0.0190	2.15
	Quảng Nam	0.0000	0.0000	0.00
	Quảng Ngãi	0.2991	0.0058	0.05
	Quảng Ninh	0.0000	0.0000	0.00
	Quảng Trị	0.1962	0.0376	1.40
	Sóc Trăng	0.0000	0.0000	0.00
	Tây Ninh	0.0000	0.0000	0.00
	Thái Bình	0.0000	0.0000	0.00
	Thanh Hóa	0.0000	0.0000	0.00
	Thừa Thiên–Huế	0.1839	0.0241	2.24
	Tiền Giang	0.0000	0.0000	0.00
	Trà Vinh	0.0000	0.0000	0.00
	Vĩnh Long	0.0000	0.0000	0.00
	All Vietnam	0.2457	0.0256	7.58

Salt	Province Name	Mean Vulnerability	Mean Risk	Expected Change by 2050 (km2)
	An Giang	0.0000	0.0000	0.00
	Bà Rịa–Vũng Tàu	0.4598	0.8003	3.04
	Bắc Giang	0.0000	0.0000	0.00
	Bạc Liêu	0.0000	0.0000	0.00
	Bắc Ninh	0.0000	0.0000	0.00
	Bến Tre	0.3348	0.4331	8.97
	Bình Định	0.0000	0.0000	0.00
	Bình Dương	0.0000	0.0000	0.00
	Bình Thuận	0.3562	0.0000	0.00
	Cà Mau	0.0000	0.0000	0.00
	Cần Thơ City	0.0000	0.0000	0.00
	Đà Nẵng City	0.0000	0.0000	0.00
	Đồng Nai	0.0000	0.0000	0.00
	Đồng Tháp	0.0000	0.0000	0.00
	Hà Nam	0.0000	0.0000	0.00

	Hà Tây	0.0000	0.0000	0.00
	Hà Tĩnh	0.0000	0.0000	0.00
	Hải Dương	0.0000	0.0000	0.00
	Hải Phòng City	0.0000	0.0000	0.00
	Hậu Giang	0.0000	0.0000	0.00
	Hồ Chí Minh City	0.2608	0.0436	0.45
	Hòa Bình	0.0000	0.0000	0.00
	Hưng Yên	0.0000	0.0000	0.00
	Khánh Hòa	0.4049	0.2839	1.89
	Kiên Giang	0.0000	0.0000	0.00
	Long An	0.0000	0.0000	0.00
	Nam Định	0.0000	0.0000	0.00
	Nghệ An	0.0000	0.0000	0.00
	Ninh Bình	0.0000	0.0000	0.00
	Ninh Thuận	0.0000	0.0000	0.00
	Phú Yên	0.0000	0.0000	0.00
	Quảng Bình	0.0000	0.0000	0.00
	Quảng Nam	0.0000	0.0000	0.00
	Quảng Ngãi	0.0000	0.0000	0.00
	Quảng Ninh	0.0000	0.0000	0.00
	Quảng Trị	0.0000	0.0000	0.00
	Sóc Trăng	0.0000	0.0000	0.00
	Tây Ninh	0.0000	0.0000	0.00
	Thái Bình	0.0000	0.0000	0.00
	Thanh Hóa	0.0000	0.0000	0.00
	Thừa Thiên–Huế	0.0000	0.0000	0.00
	Tiền Giang	0.0000	0.0000	0.00
	Trà Vinh	0.0000	0.0000	0.00
	Vĩnh Long	0.0000	0.0000	0.00
	All Vietnam	0.3375	0.3483	14.35

Discussion and Conclusions

The multi-layer perceptron was used in producing the vulnerability maps because of previous experience that has shown it to be a strong and consistent performer (Eastman et al., 2005). Although no standard has been established for the skill of empirical models of land cover change, it is our general experience that any skill above 0.5 is good. All of the models used in this study exceeded that threshold.

When the multi-layer perceptron is coupled with case-control sampling where equal-sized samples of change and persistence are used, it produces an output whose character can best be described as vulnerability. In reality, it expresses the posterior probability of transition assuming equal prior probability. This can usefully be thought of as a statement of vulnerability irrespective of the rate of change. By applying a Bayesian *prior* correction the same vulnerability map can be used to create multiple maps of risk assuming varying rates of change. Planners can thus identify areas that are vulnerable and evaluate the effect of varying interventions.

Each of the two kinds of map has advantages and disadvantages. The vulnerability map does not consider the rate of change associated with the transition while the risk map does. This would seem to be a distinct advantage of the risk map. However, the units on the risk map are awkward. They express the probability that a specific pixel will transition. By simply changing the resolution, that number will change. There is no meaning to the probability expressed on the risk map without consideration of the resolution. The vulnerability map, however, always has the same character regardless of the resolution. The number is also easy to understand. Finally, the relationship between vulnerability and risk is non-linear, and increasingly so as the rate becomes very small or very large. In the context of land cover change, the rates will typically be quite small. In these cases, the contrast between varying probabilities will be quite small, as is apparent in the main mangrove area in Figure 2.

Coastal land cover is clearly undergoing enormous change in Southeast Asia related to expansion of aquaculture. Over the region as a whole, the area of pond aquaculture has increased over 400%. Clearly there needs to be better planning for this kind of rapid change. We expect that maps of vulnerability and risk as introduced in this study can make a major contribution to such an effort.

References

Abdus Salam, M., Ross, L., and Beveridge, C.M. (2003) A comparison of development opportunities for crab and shrimp aquaculture in southwestern Bangladesh, using GIS modeling. *Aquaculture*, 220, 477-494. doi:10.1016/S0044-8486(02)00619-1.

Anh Duc, N., (2008) *Salt Intrusion, Tides and Mixing in Multi-channel Estuaries*. (Leiden, The Netherlands: Taylor and Francis/Balkema).

Arli, P., (2007) *Numerical Modeling of possible Saltwater Intrusion Mechanisms in the Multiple-Layer Coastal Aquifer System of the Gulf of Thailand*. (Germany: Kassel University Press).

Barbier, E. B., and M. Cox. 2004. “An Economic Analysis of Shrimp Farm Expansion and Mangrove Conversion in Thailand.” *Land Economics*, 80(3), 389-407. doi: 10.2307/3654728.

Cardona, O.D., (2003) The Need for Rethinking the Concepts of Vulnerability and Risk from a Holistic Perspective: A Necessary Review and Criticism for Effective Risk Management, in *Mapping Vulnerability: Disasters, Development and People*, G. Bankoff, G. Frerks, D. Hilhorst (Ed), (London: Earthscan Publishers).

Chavez, P. S., (1996) Image-Based Atmospheric Corrections - Revisited and Improved, *Photogrammetric Engineering and Remote Sensing*, 62, 1025-1036.

Dahdouh-Guebas, F., T. Zetterström, P. Rönnbäck, M. Troell, A. Wickramasinghe, and N. Koedam. 2002. “Recent changes in land-use in the Pambala-Chilaw lagoon complex (Sri Lanka) investigated using Remote Sensing and GIS: Conservation of mangroves vs. development of shrimp farming.” *Environment, Development and Sustainability*, 4, 185-200.

Eastman, J.R., Crema, S.C., Sangermano, F., Cunningham, S., Xiao, X., Zhou, Z., Hu, P., Johnson, C., Arakwiye, B., Crone, N., (forthcoming) A Baseline Mapping of Aquaculture and Coastal Habitats in Thailand, Cambodia and Vietnam.

Eastman, J.R., (2015) *TerrSet Geospatial Monitoring and Modeling System*, (Worcester, MA: Clark Labs).

Eastman, J.R., Van Fossen, M. E. and Solorzano, L.A., (2005) Transition Potential Modeling for Land Cover Change, Chapter 17 in *GIS, Spatial Analysis and Modeling*, D. Maguire, M. Batty, and M. Goodchild, eds., (Redlands, California : ESRI Press), 357-386.

Foody, G.M., Campbell, N.A., Trodd, N.M., and Wood, T.F., (1992) Derivation and Applications of Probabilistic Measures of Class Membership from the Maximum Likelihood Classification, *Photogrammetric Engineering and Remote Sensing*, 58, 9, 1335-1341.

Giap, D., Yi, Y., and Yakupitiyage, A., (2005) GIS for land evaluation for shrimp farming in Haiphong of Vietnam. *Ocean & Coastal Management*, 48(1), 51-63. doi: 10.1016/j.ocecoaman.2004.11.003.

Grimstead, C.M., and Snell, J.L., (1997) Markov Chains, Chapter 11 in *Introduction to Probability*, 2nd Edition, (Providence, RI: American Mathematical Society).

Hsieh, W.W. (2009) *Machine Learning Methods in the Environmental Sciences: Neural Networks and Kernels*, (NY: Academic).

King, G., and Zeng, L. (2001a) Logistic Regression in Rare Events Data. *Political Analysis* 9, 137–163

King, G., and Zeng, L. (2001b) Explaining Rare Events in International Relations. *International Organization* 55: 693–715

Lebel, L., H. T. Nguyen, A. Saengnoree, S. Pasong, U. Buatama, and L. K. Thoa. 2002. "Industrial Transformation and Shrimp Aquaculture in Thailand and Vietnam: Pathways to Ecological, Social, and Economic Sustainability?" *Ambio*, 31(4), 311-323.

Li, Z. and Fox, J., (2010) Integrating Mahalanobis typicality with a neural network for rubber distribution mapping. *Remote Sensing Letters*, 2(2), 157-166. doi: 10.1080/01431161.2010.505589.

McLeod, I., Pantus, F. and Preston, N., (2002) The use of a geographical information system for land-based aquaculture planning. *Aquaculture Research*, 33(4), 241250. doi: 10.1046/j.1355-557x.2001.00667.x.

Rogan, J., and Yool, S., (2001) Mapping fire-induced vegetation depletion in the Peloncillo Mountains, Arizona and New Mexico. *International Journal of Remote Sensing*, 22(16), 3101-3121.

Szuster, B.W. 2006. “Coastal Shrimp Farming in Thailand: Searching for Sustainability.” *Environment and Livelihoods in Tropical Coastal Zones*, 86-98.

Vo, Q. T., N. Oppelt, P. Leinenkugel, and C. Kuenzer. 2013. “Remote Sensing in Mapping Mangrove Ecosystems—An Object-Based Approach.” *Remote Sensing*, 5, 183-201. doi: 10.3390/rs5010183.

Vu M.C., Bui D.D., (2006) Assessment of Saline Water Intrusion into Estuaries of Red-Thai Binh River during Dry Season Having Considered Water Released from Upper Reservoirs and Tidal Fluctuation. Japan - Vietnam Estuary Workshop, the Water Resources University.

Weiss, G.G., (2004) Mining with rarity: A Unifying Framework, *SIGKDD Explorations*, 6, 1, 7-19.

Zhu, Z., Wang, S., and Woodcock, C., (2015) Improvement and Expansion of the Fmask Algorithm: Cloud, Cloud Shadow, and Snow Detection for Landsats 4-7, 8, and Sentinel 2 Images. *Remote Sensing of Environment*, 159, 269-277.